

Interpreting the signal from a localized fluorescence sensor: a study by angle-resolved XPS and dynamic SIMS [☆]

Dara L. Woerdeman,^{a,*} Wei Ou,^b Joseph L. Lenhart,^{c,1} and Richard S. Parnas^d

^a Metallurgy & Materials Engineering Department, Katholieke Universiteit, 44 Kasteelpark Arenberg, B-3001 Heverlee, Belgium

^b Materials Characterization Group, Evans East, East Windsor, NJ 08520, USA

^c Polymers Division, National Institute of Standards & Technology, Gaithersburg, MD 20899, USA

^d Institute of Materials Science, University of Connecticut, Storrs, CT 06269, USA

Received 21 May 2002; accepted 28 January 2003

Abstract

Angle-resolved X-ray photoelectron spectroscopy (XPS) and dynamic secondary ion mass spectroscopy (DSIMS) experiments were conducted to assess the interactions between a diamine curing agent and a glycidoxysilane-modified glass substrate. This effort was motivated by earlier work, in which a fluorescent probe localized in dilute quantities in the silane layer was used to track the penetration of the resin into the silane layer, as well as the resin cure. XPS and DSIMS experiments were performed on the silane layers immersed only in the resin hardener, providing more detailed information about the concentration profile and structural reorganization within the silane layer due specifically to hardener penetration. Dynamic SIMS spectra reveal the presence of hardener in the layer, as indicated by the strong CN⁻ signal throughout the silane layer thickness. The XPS results indicate the presence of an amine gradient within the top 10 nm of the silane coating, with less amine penetration deeper into the silane layer. The XPS data also suggest some level of anisotropy in the molecular structure of the diamine/glycidoxysilane coating, as revealed by the differences in the relative atomic concentrations and peak positions of the C1s components at two different take-off angles.

© 2003 Elsevier Science (USA). All rights reserved.

Keywords: Angle-resolved XPS; SIMS; Glycidoxysilane; Fluorescent probe; Organosilanes; Glass/epoxy interface; Silane-modified glass

1. Introduction

Polymer interfaces are critical to the function of composite materials, since the interfacial region either controls or plays a major role in determining several composite properties such as flexural strength and durability [1–3]. The properties of composite interfaces are not well understood, however, due to the difficulty of taking measurements at sub-micrometer length scales often inaccessible with standard measurement techniques. It is also widely recognized that

surface-induced perturbations can propagate away from a fiber surface to induce the formation of a three-dimensional zone with properties different from those of the bulk polymer (often referred to as the interphase), particularly for fibers coated with a finish or coupling agent [4]. For example, concentration gradients can arise if one of the reacting components of the resin mixture has a higher affinity for the fiber surface than the other components. Therefore, the challenge lies in understanding the effects of surface-induced perturbations on properties such as the glass transition temperature, strength, and fracture toughness.

Indirect evidence of the property differences between the interphase zone and the bulk matrix has been obtained with techniques such as single filament fragmentation measurements, microindentation measurements, and fiber pull-out measurements [5–7]. Nevertheless, the minute dimensions of the interphase zone make it difficult to acquire direct *in situ* measurements of its properties [8,9].

Chemically grafting a fluorescent probe onto an organosilane-modified glass surface has proven to be an effective way to monitor the chemical and physical properties of the buried

[☆] Certain commercial equipment, instruments, or materials are identified in this paper in order to specify the experimental procedure adequately. Such identification is not intended to imply recommendation or endorsement by the National Institute of Standards and Technology, nor is it intended to imply that the materials or equipment identified are necessarily the best available for the purpose.

* Corresponding author.

E-mail addresses: Dara.Woerdeman@mtm.kuleuven.ac.be (D.L. Woerdeman), jllenha@sandia.gov (J.L. Lenhart).

¹ Current address: Sandia National Laboratory, Albuquerque, NM 87185, USA.

polymer/glass interfacial region [10–12]. In particular, the fluorescent dye is localized on the substrate surface, and therefore the fluorescence response is sensitive only to the interphase region rather than the bulk polymer [10–12]. What makes localized fluorescence spectroscopy so attractive is its versatility, and the potential one has to integrate it with fiber-optic evanescent wave spectroscopy [13–15], permitting the characterization of polymer interfaces that exist in an actual composite part.

This recent work has succeeded in measuring the fluorescence behavior of epoxy/silane coatings on silica surfaces. However, one disadvantage of the technique is that the fluorescent response is collected from the entire region containing the dye. As a result, the average properties of the interfacial region are measured without spatial resolution. The present work complements the previous fluorescence studies by providing much more detailed chemical and elemental profiles in a model diamine/epoxy-terminated organosilane system on glass. In addition, the surface analysis measurements presented in this paper are intended to shed light on the true significance of the fluorescent response from the grafted dye.

Therefore, the goal of the work is twofold: First, to elucidate the structure of the silane coupling agent layer/resin interfacial region, and second, to better understand the physical significance of the fluorescence response obtained from the probe grafted within the silane layer. The localized fluorescence sensor is immersed in an epoxy resin and the fluorescent response is measured during the course of resin cure (Fig. 1). While the fluorescence sensor indicates significant resin penetration into the silane layer and can potentially be correlated with the interfacial extent of cure, several questions remain unanswered. For example, it is unknown whether the fluorescent dye in the silane deposition solution

influences the resulting thickness of the silane layer on the glass substrate, even though it is present in minute quantities. Second, up to now, it has been assumed that the fluorescent response measures the extent of reaction between the epoxy end groups of the silane layer and the amine hardener molecules in the vicinity of the surface. But it remains unclear to what extent the hardener molecules penetrate the organosilane interlayer and react with the silane end groups. In addition, the concentration profile of the resin monomers within the silane layer is unknown, since the fluorescent response is averaged over the entire coupling agent layer. Other issues relate to how the organosilane can reorganize in the presence of the amine hardener. For example, does the amine-curing agent change the dimensions of the silane coating? Is molecular reorientation of the glycidoxysilane interlayer induced by the presence of a diamine overlayer?

To address these additional issues and to provide further insight into the structure of the coupling agent/resin interfacial region, angle-resolved XPS experiments were conducted on these layers. An important goal was to learn how the presence of the resin could influence the structure of the underlying organosilane coating. Dynamic SIMS experiments were also performed to determine the level of interpenetration between the silane layers and the amine-curing agent. Comparisons of layer thickness were made between two sets of samples: (1) dye-doped and undoped glycidoxysilane layers, and (2) plain and diamine-coated glycidoxysilane layers. The four sets of data could not be compared directly since nitrogen was used as the elemental probe in both studies, to track either the presence of the dye in the silane layer or the diffusion of the amine-curing agent into the glycidoxysilane coating.

2. Experimental

2.1. Preparation of fluorescent thin films

For the purpose of achieving true interfacial sensitivity, the fluorescent probe molecules were chemically anchored to the glass surface. In particular, the fluorophore, dimethylaminonitrostilbene (DMANS), was tethered to a triethoxysilane coupling agent, giving rise to a fluorescent labeled silane coupling agent (FLSCA) molecule, depicted in Fig. 2. The details of the chemistry performed in tethering the fluorophore to the organosilane have been described in earlier work [10,11]. In an effort to minimize the intrusiveness of the fluorescent probe molecules, as well as to optimize their fluorescent emission intensity, the FLSCA was diluted with a different silane coupling agent prior to deposition. In the present work, the diluting silane coupling agent was glycidoxypropyltrimethoxysilane (GPS) (Fig. 3); therefore the silane layer deposited on the glass substrate consisted primarily of GPS molecules, intermingled with a low concentration of FLSCA probe molecules, as recapped below [10,11].

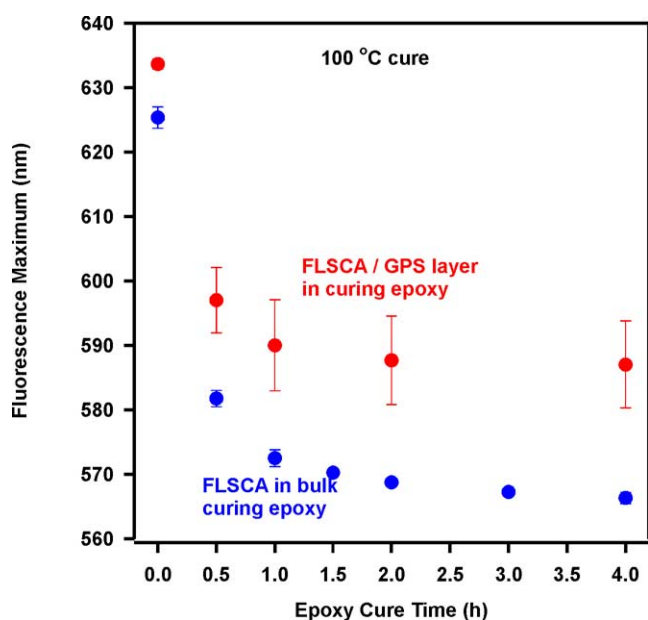


Fig. 1. The changing fluorescence signal during epoxy cure.

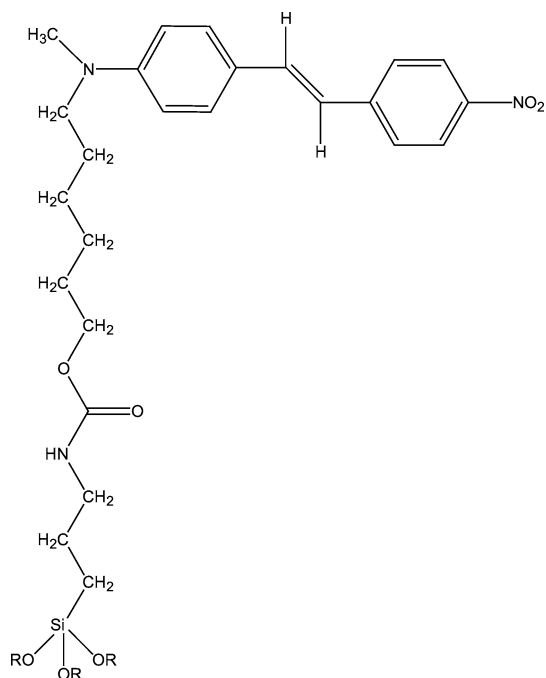


Fig. 2. Fluorescent-labeled silane coupling agent (FLSCA) molecule is formed by chemically attaching the (dimethylamino)nitrostilbene fluorophore to triethoxysilane.

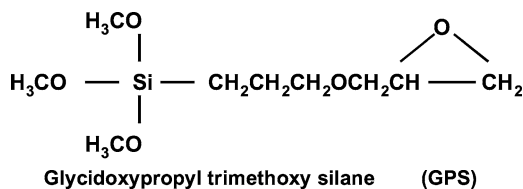


Fig. 3. Chemical structure of the epoxy-terminated silane coupling agent glycidoxypropyltrimethoxysilane (GPS).

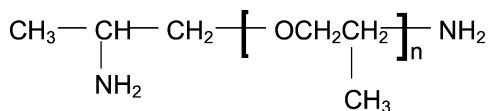


Fig. 4. Chemical structure of the diamine hardener Jeffamine D230. The “*n*” is adjusted so that the number-average molecular weight of the curing agent is 230 g/mol.

GPS and FLSCA were added to an ethanol/water mixture with a volume fraction of ethanol equal to 95%, under slightly acidic conditions. The molar ratio of FLSCA to GPS was 0.006 in the samples analyzed in this work. (However, for samples that included the diamine-curing agent, the fluorescent dye was intentionally left out of the organosilane layer to avoid any ambiguity in the analysis of the nitrogen signal.) After hydrolysis of the organosilanes, clean glass microscope cover slips were immersed in the deposition solution for 10 min. The total organosilane concentration in the deposition solution was set at 0.2 mmol/ml in this study.

The coated cover slips were cured at $100 \pm 2^\circ\text{C}$ for 1.5 ± 0.2 h and subsequently washed by two successive dips in clean ethanol for 30 ± 5 s. After drying for roughly an hour

at 100°C , the samples were sealed in a glass vial and stored in the dark. The model interface was created by allowing the GPS-modified or GPS/FLSCA-modified slide to react with a linear diamine hardener, Jeffamine D230 (Fig. 4), at 100°C for 20 h. The slides were subjected to an acetone rinse to remove unreacted hardener prior to conducting the surface analysis experiments.

2.2. X-ray photoelectron spectroscopy measurements

The XPS analysis was carried out using a SPECS spectrometer equipped with a standard $\text{AlK}\alpha$ X-ray source ($h\nu = 1486.6$ eV, anode voltage 15 kV, filament current 20 mA, power 250 W). For the survey-scan spectra, a pass energy of 30 eV, a step size of 0.2 eV, a dwell time of 50 ms, and a scan total of 1 were selected, while for high-resolution scans, these parameters were set at 30 eV, 0.1 eV, 1 s, and 7, respectively. Spectra were collected over a 1.0-mm-diameter spot analysis area with the sample surface oriented at either 90° or 40° relative to the analyzer lens. The sampling depths at the 90° and 40° electron take-off angles were estimated to be 5–10 and 3–7 nm, respectively [16]. Signal collection utilized a 180° hemispherical analyzer in the constant analyzer energy mode. The signal was digitized and processed using SpecsLab 1.8.2 ESCA software. The aliphatic component of the $\text{C}1\text{s}$ peak (285 eV) was used as a binding energy reference.

2.3. Dynamic SIMS measurements

The experiments were performed using a Physical Electronics Model 6600 quadrupole SIMS system. The instrument is equipped with a cesium ion source for the detection of electronegative elements. Sputtering was accomplished by continuously sputtering away the sample surface while monitoring the ions of interest. In the current work, the N, C, Si, and O secondary ion profiles were plotted in intensity units (counts/s) versus sputtering depth (micrometers). For the thicker coatings (0.4–0.8 μm), depth scales were determined by measuring, with a calibrated Tencor Alpha Step 200 profilometer, the depths of a few craters sputtered into the thin film specimens. The profilometry measurements had a relative standard deviation of 3%. However, for the thinner films (< 0.4 μm), it was not possible to develop a reliable calibration of thickness versus ion beam sputtering time. Therefore intensity measurements on these films are presented as a function of film ablation time (s).

3. Results and discussion

3.1. Angle-resolved XPS studies: amine profile as a function of depth

To study the potential impact of a resin overlayer on the silane layer structure near the coupling agent/resin interface,

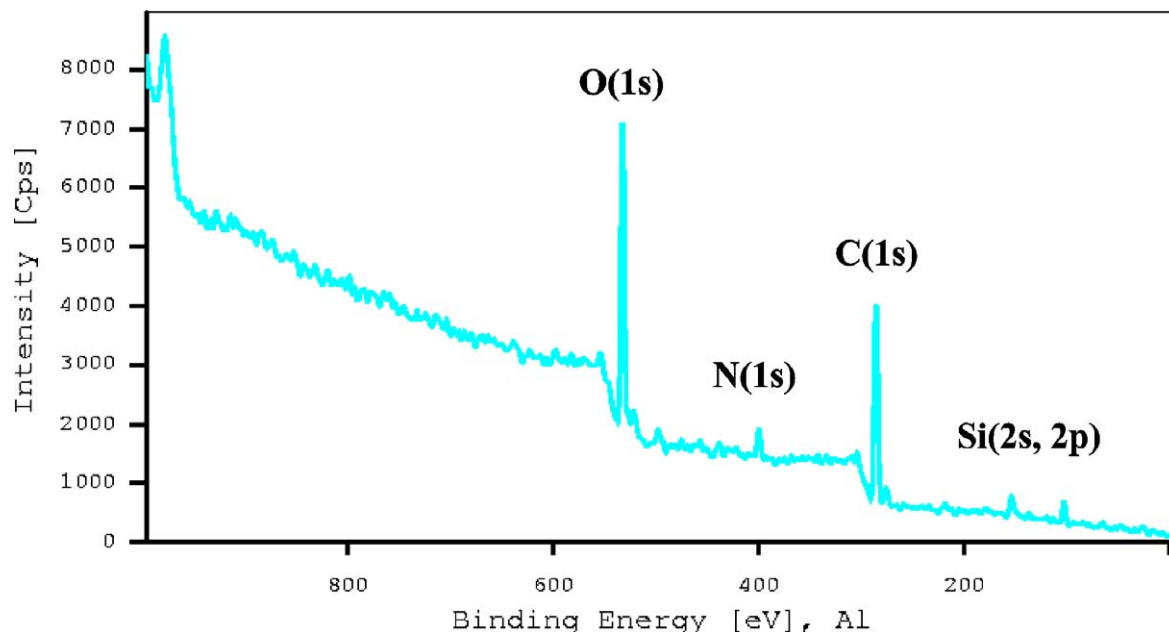


Fig. 5. XPS survey spectrum of the GPS/Jeffamine D230 film at a 90° electron take-off angle.

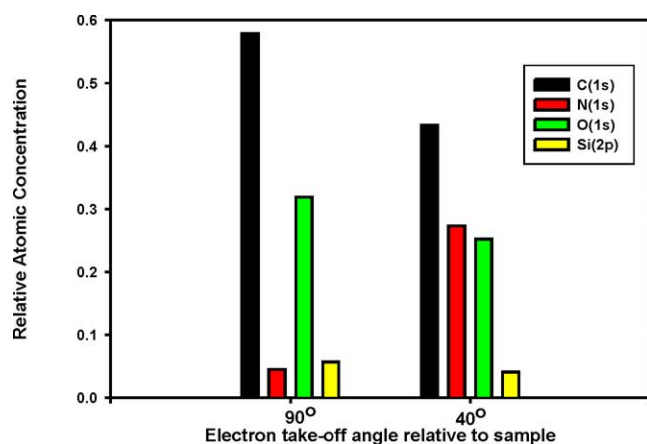


Fig. 6. Tabulation of the angle-resolved XPS data for a GPS/Jeffamine D230 film. The relative atomic concentrations of carbon, nitrogen, oxygen, and silicon are presented from spectra acquired at two take-off angles: 90° (sampling depth 5–10 nm) and 40° (sampling depth 3–7 nm).

angle-resolved XPS studies were conducted on GPS layers immersed in resin hardener. An XPS survey scan (acquired at a 90° take-off angle) of the GPS/Jeffamine D230 model interface is depicted in Fig. 5. Most of the physisorbed diamine was removed by the acetone soak, as indicated by the discernible Si2s and Si2p peaks (GPS signatures) in the spectrum (Fig. 5). Moreover, the spectrum suggests that the GPS molecules were interdispersed with the diamine molecules in the top 10 nm of the film, as the relative atomic concentrations of both N (a signature of the Jeffamine curing agent) and Si ranged from 3 to 30% (Fig. 6). The atomic concentration of each of the four elements was normalized against the combined concentration of the four elements (C, N, O, Si).

As shown in Fig. 6, angle-resolved XPS was conducted at two different electron take-off angles to provide a rough estimate of the surface composition profile of the GPS/Jeffamine D230 film within the top 10 nm of the surface. It is important to remember that while all atoms within the path of the probing X-ray contribute to the XPS signal, the contribution of each atom decreases exponentially with the distance from the free surface [17]. As a result, the convoluted nature of the signal distorts depth profiles for samples with compositional gradients. However, the angle-resolved XPS spectra clearly indicate the existence of an amine gradient in the top few nanometers of the film (40° take-off angle, relative concentration of N measured as 0.3), with less amine penetration further into the layer (90° take-off angle, relative concentration of N measured as 0.03).

These angle-resolved XPS data complement the external reflection Fourier transform infrared spectroscopy (FTIR) measurements made previously on the same model glass/epoxy interface [18]. The combination of the XPS and FTIR data not only demonstrate that the amine hardener was able to penetrate into the layer, but also suggest a reaction between the amine on the curing agent and the epoxide on the GPS, as evidenced by the disappearance of the strained CH stretching modes in the FTIR spectrum, associated with the epoxide functionality on GPS [18].

3.2. Angle-resolved XPS studies: effect of amine hardener on structure of GPS layer

Angle-dependent XPS studies were also conducted to aid in the analysis of the GPS layer in the presence of the Jeffamine D230 overlayer. As has been proposed previously, the presence of an overlayer can potentially induce ordering in the underlying film at a distance of several

nanometers from the interface [19]. Angle-resolved XPS is often used to investigate the various chemical states of each element present in a system. In the present work, we analyzed the C1s signal to gain initial understanding of the GPS/Jeffamine D230 film structure. To avoid overfitting the data, we did not attempt to account for all possible chemical environments involving carbon; however, we performed a partial deconvolution of the C1s peak, as described below.

Partial deconvolution of the C1s peak in the spectra acquired at the two take-off angles, 90° and 40° (Figs. 7a and 7b, respectively), was achieved using a standard non-linear least-squares fitting routine (Levenberg–Marquardt method) [20]. For both angles, the curve fit generated two broad peaks, each encompassing a variety of chemical states.

In a related study by Abel et al. [21] involving interactions between GPS and a diamine-curing agent [21], the carbon signal was also peak fitted with two components. In particular, the first peak was set at 285 eV for internal reference, while the second component exhibited a chemical shift ranging from 1.6 to 2.0 eV, which they attributed to oxidized carbon species ranging from alcohol to epoxy functionality [21].

According to Briggs and Seah [16], carbon bound to itself and/or hydrogen only gives C1s = 285.0 eV, while oxygen induces shifts to higher binding energy by approximately 1.5 eV per C–O bond. C bonded to a secondary or tertiary amine group, however, is only expected to induce a shift in the range of 0.2–0.4 eV [16].

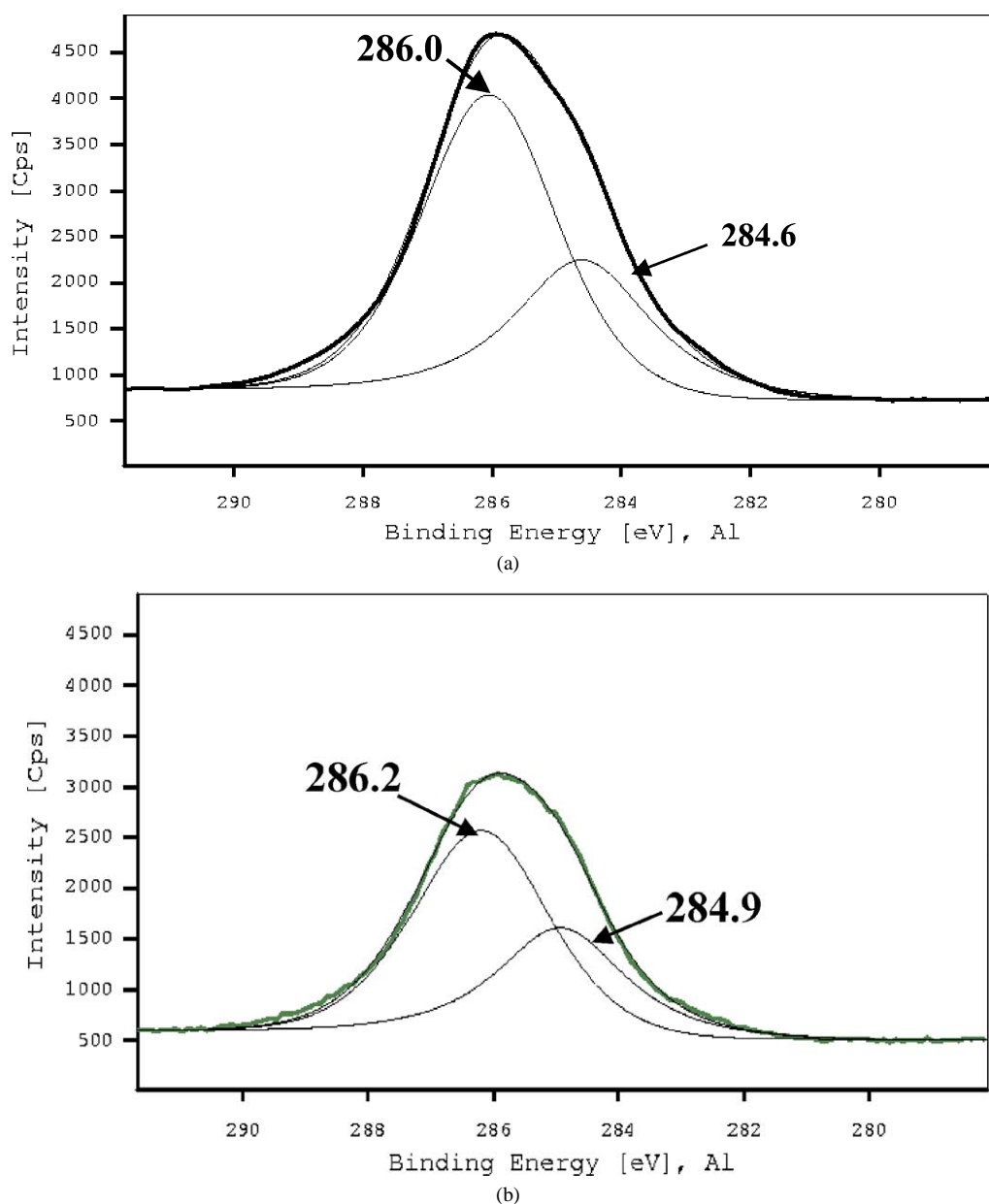


Fig. 7. High-resolution XPS scans of peak-fitted C1s signal, exhibiting a partial deconvolution of the chemical states. (a) Spectrum acquired at a 90° take-off angle. (b) Spectrum acquired at a 40° take-off angle.

In the C1s spectrum acquired at the 90° electron take-off angle, the peak maxima were at 284.6 and 286.0 eV (Fig. 7a). In Fig. 7b, which depicts the more surface-sensitive spectrum acquired at a 40° take-off angle, the C1s peaks were shifted to 284.9 and 286.2 eV. According to information in [16], one can presume that the peaks at 286 eV represent the C–O bonds in the system. In both Figs. 7a and 7b, the area of the peak at the higher binding energy (286 eV) was twice that of the lower energy peak, which is not surprising considering the large number of C–O bonds that exist in the molecular network of the diamine/GPS film. As was discussed earlier, the strong N signal in Fig. 5 suggests that a significant portion of the Jeffamine D230 curing agent was present in the top 10 nm of the coating. Along the same lines, we believe that the differences in the C1s peak positions Figs. 7a and 7b further supports our hypothesis of a concentration gradient in the top 10 nm of the film.

Similarly, the binding energies 0.2–0.3 eV shift lower as a function of depth could be indicative of some sort of GPS gradient, with more C–O bonds residing among the outermost layers of the film and with more of the aliphatic carbons residing deeper in the layer. One should be reminded that the glycidoxy or oxirane functionality is composed largely of C–O bonds, and that the oxidated species give rise to the higher energy peaks [16,21]. With this in mind, it is certainly possible that the interpenetrating diamine molecules induced some degree of reorientation in the polar GPS film during swelling [22]. Dynamic SIMS experiments were performed on this model glass/epoxy interface to shed additional light on this question of swelling.

3.3. Dynamic SIMS studies: characterizing interactions between amine hardener and glycidoxysilane interlayer

Since the fluorescence measurement (Fig. 1) has no spatial resolution, DSIMS was performed on GPS layers immersed in hardener to estimate the extent of interpenetration possible between the coupling agent and hardener molecules. Figures 8a–8c depict representative plots of the profiles obtained on the layers (a Jeffamine D230/GPS film, a plain GPS film, and unmodified glass, respectively), and the thickness measurements for this entire series of experiments are summarized in Table 1. The N, C, Si, and O secondary ion profiles are presented in intensity units (counts/s) versus depth (micrometers). The N profiles, as determined by the CN^- secondary ion intensity, have been normalized to account for variations resulting from changes in sample position from one analysis to another. As a general rule, a change in the intensity caused by instrumental factors can be minimized by normalization. Therefore, a relative comparison in the N profile among the plots should be valid for evaluating their respective N content.

The results reveal that the N signal (extracted from the measured CN^- concentration) is nearly 100 times more intense in the spectrum of the *GPS/D230 hardener* sample

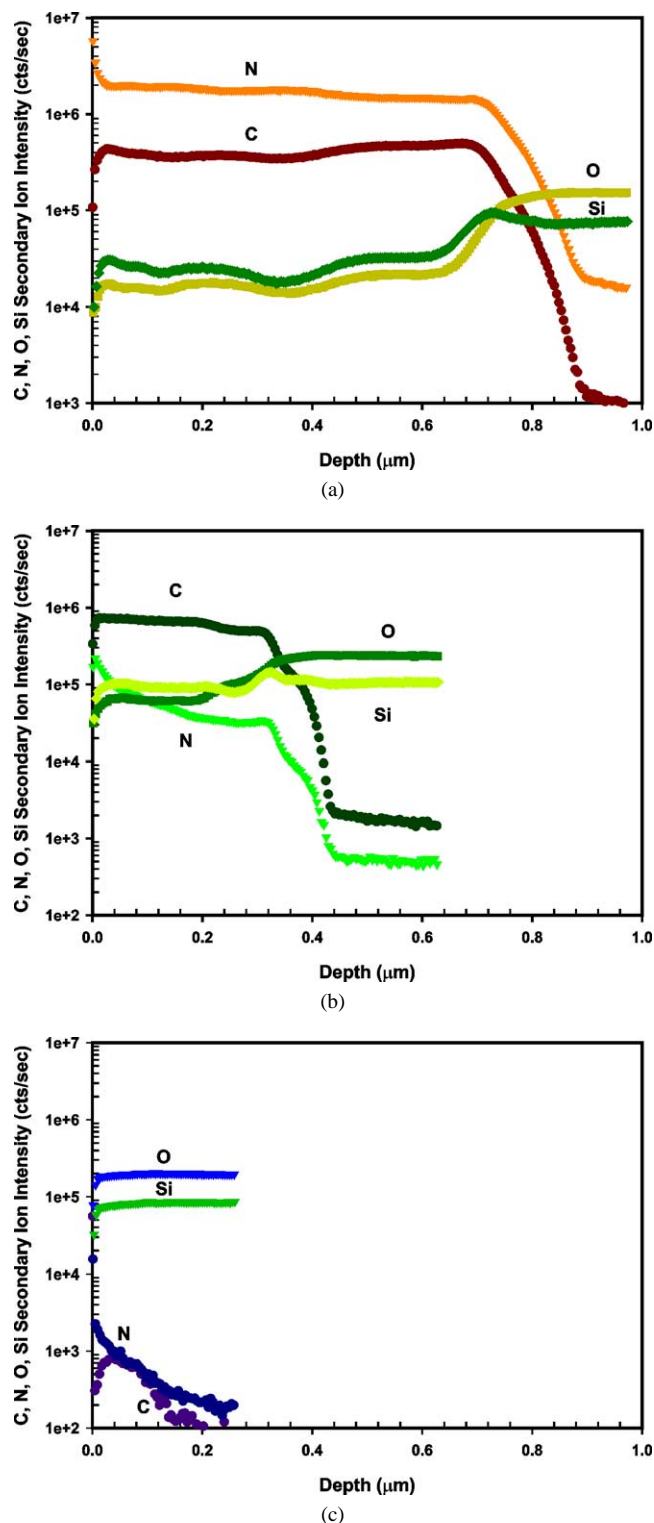


Fig. 8. Dynamic SIMS depth profiles. C, N, O, Si secondary ion intensities (counts/s) plotted as a function of sampling depth (μm). (a) Jeffamine D230/GPS film. (b) GPS control film. (c) Plain glass.

(Fig. 8a) than in the spectrum of the *GPS* control sample (Fig. 8b). This result is consistent with the expectation of hardener retention in the *GPS/D230 amine hardener* sample. The presence of N can be tracked throughout the entire

~0.7 μm GPS/D230 hardener coating and thus suggests its presence throughout the layer, even if present only in remote quantities. (Recall that with SIMS one can detect the presence of fragment ions in ppm or ppb.) Repeat measurements were taken on two additional samples to provide an estimate of the level of reproducibility in these measurements ($\pm 0.05 \mu\text{m}$).

Though the less intense N signal detected in the ~0.35- μm surface layer of the GPS control sample is suggestive of the presence of N, the apparent N signal ($^{12}\text{C}^{14}\text{N}^-$) may contain an interference contribution from $^{12}\text{C}^{13}\text{CH}^-$ or $^{12}\text{C}^{12}\text{CH}_2^-$ having the same nominal secondary ion mass as $^{12}\text{C}^{14}\text{N}^-$. The quadrupole mass spectrometer utilized does not have sufficient mass resolution to discriminate between the hydrocarbon signals and N. Therefore, the N profiles for both samples may be due in part to hydrocarbon, which is omnipresent for GPS. If one takes the GPS control to set the baseline for the hydrocarbon contribution to the apparent N profile, the GPS in D230 hardener sample, with its significantly more intense N signal, would still have an additional N (i.e., amine hardener). This evaluation assumes that the hydrocarbon background level for both samples is the same, which should be valid since both organic film layers are composed mostly, 99%, of GPS. As a control experiment, a scan was performed on a blank glass microscope slide (Fig. 8c), but no significant amount of carbon contamination was detected on the surface of the glass.

There is still the question of whether the Jeffamine D230 curing agent swells the GPS layer as a result of penetration. The thickness measurements of the GPS coating with and without the Jeffamine D230 overlayer can be found in Table 1. As the thickness of a GPS coating was found to vary by as much as 50% [10–12], we conducted a null hypothesis test to explore whether the observed differences in layer thickness were statistically significant. If the thickness variations between the two data sets are statistically insignificant (our null hypothesis), the mean film thickness for all six samples is calculated as 0.56 μm with a standard deviation of 0.22 μm . This gives rise to a standard error of 0.90 and a z -score of 2.2. The null hypothesis is therefore proven false at a 0.05 level of significance, or alternatively, one can state with at least 95% certainty that the measured thickness differences between the two sets of

samples (GPS-coated and GPS/Jeffamine D230-coated) are statistically significant (Table 1).

3.4. Dynamic SIMS studies: effect of fluorescent probe on organosilane layer thickness

The results for the two *fluorescent-dye-doped GPS* samples (Table 2) suggest that there is N present within the carbonaceous surface film of these two samples. The GPS control samples (Fig. 9a, Table 2) exhibited carbonaceous surface layers thinner than those of the two *fluorescent-dye-doped GPS* samples (Fig. 9b, Table 2). It is possible that the addition of small amounts of the DMANS fluorescent dye (fluorescent dye/GPS ratio of 1/125) contributes to the formation of a gel layer, as others have observed that amine groups present in the silane system have the potential to catalyze the organosilane deposition reaction [23].

Previous studies have demonstrated that a wide variety of factors can influence depositions, leading to irreproducible organosilane coatings, including, for example, the temperature, the solvent, and its water content [24]. De Boer et al. [25] also point out that even once the layers are deposited, coating properties can continue to change in response to a change in environmental conditions (e.g., an increase in humidity). More specifically, surface structures can rearrange to form alternate phases, and these aggregates can be incorporated into film structures, contributing to irreproducible film properties [24].

Although the fluorescent dye could have led to an increase in silane layer thickness or surface roughness, it has been shown that the presence of dopant quantities of dye molecules in the silane layer will not interfere with the cure kinetics of the GPS/amine hardener system [10]. Therefore, if desired, any excess gel layer present on the sensor surface could simply be removed prior to embedding the sensor in an actual composite. In addition, the FLSCA/GPS ratios used in this study are quite high, nearly 1 mol% FLSCA. It is certainly possible for these dye concentrations that the amine will catalyze the condensation reaction and GPS absorption. However, it is likely that more dilute FLSCA concentrations will have a lesser influence on the silane layer structure. The FLSCA concentration dependence on the silane layer struc-

Table 1

Summary of dynamic SIMS experiments performed to confirm the presence of the amine-curing agent in the silane layer and to independently characterize the structure of a GPS/Jeffamine D230 film

Sample trial number	Surface treatment	Film thickness
1	plain glass	< 0.01 μm
2A	GPS	0.38 \pm 0.05 μm
2B	GPS	0.43 \pm 0.05 μm
2C	GPS	0.37 \pm 0.05 μm
3A	D230 hardener over GPS	0.80 \pm 0.05 μm
3B	D230 hardener over GPS	0.75 \pm 0.05 μm
3C	D230 hardener over GPS	0.70 \pm 0.05 μm

Table 2

Summary of dynamic SIMS experiments conducted to determine the effect of the immobilized fluorophore in determining overall film thickness

Sample trial number	Surface treatment	Sputter time
1A	GPS + dye	260–280 s
1B	GPS + dye	100 s
1C	GPS + dye	650–680 s
1D	GPS + dye	600 s
2A	GPS	20–30 s
2B	GPS	20–30 s
2C	GPS	20–30 s
3A	GPS	10–20 s
4A	GPS + dye	300 s
4B	GPS + dye	350 s

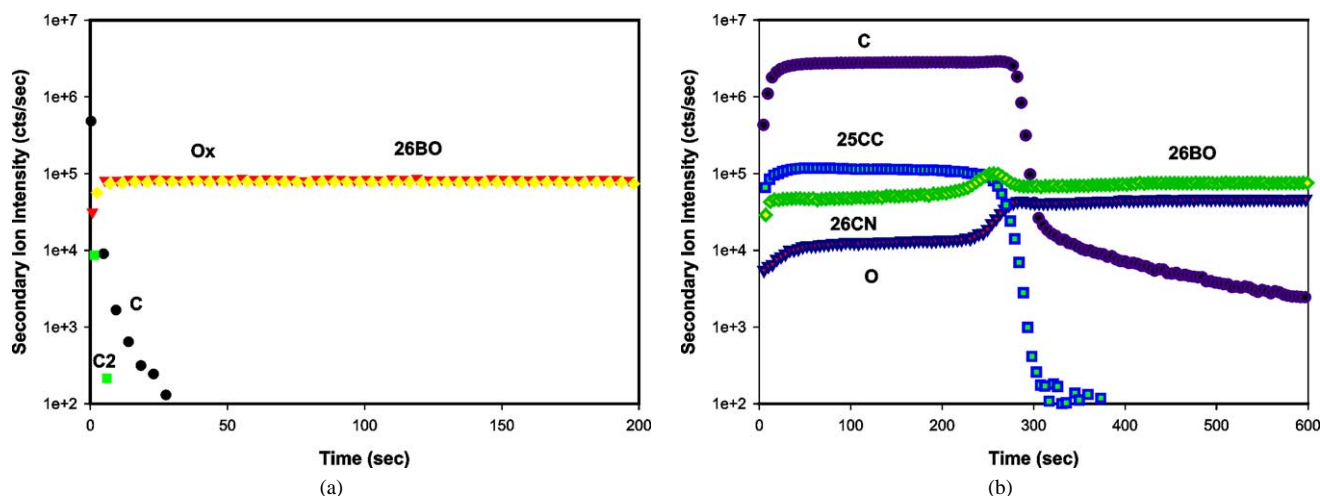


Fig. 9. Dynamic SIMS depth profiles. C, N, O, Si secondary ion intensities (counts/s) plotted as a function of sputter time (s). (a) GPS control film. (b) DMANS-doped GPS film.

ture is being investigated further. In addition, we are interested in using localized fluorescent probes with significantly higher quantum yields than FLSCA. The FLSCA quantum yield is less than 0.01. We hope to identify polarity and mobility sensitive probes with quantum yields of near 1, which will dramatically increase the interfacial signal. As part of our selection criteria for new probes, we will certainly focus on the potential influence of the probe on the interfacial structure.

4. Summary

Angle-resolved XPS and dynamic SIMS experiments were performed as part of a larger study to understand the chemical and physical interactions between an amine curing agent and a glycidoxysilane layer on a silica surface. Sensor technology based on localized fluorescence spectroscopy has recently been developed to measure the properties of buried glass/epoxy interfaces, and the results presented in this paper should aid in the interpretation of these fluorescence measurements.

Angle-resolved XPS results on model amine/epoxy-silane systems suggest the presence of an amine gradient with less amine penetration deeper into the silane layer. Dynamic SIMS spectra reveal the presence of N in the layer, as indicated by the strong CN^- signal, with an exponential decrease in the N signal at the surface. Angle-resolved XPS data clearly illustrate that the curing agent is concentrated at the surface, as revealed by the differences in the relative atomic concentrations and peak positions of the $C1s$ components at two different electron take-off angles. Finally, results show that the low concentration of fluorophore in the silane deposition solution can potentially act as a catalyst during the silanization reaction, resulting in increased silane layer thickness or roughness.

Acknowledgment

D.L.W. thanks Dr. Ed Gillman of the Jefferson Labs. for permitting her access to the ESCA equipment in his laboratory.

References

- [1] J.L. Thomason, *Composites* 26 (1995) 427.
- [2] K.A. Lindsey, C.D. Rudd, M.J. Owen, *J. Mater. Sci. Lett.* 14 (1995) 942.
- [3] H. Ishida, *Polym. Compos.* 5 (1984) 101.
- [4] B.K. Fink, R.L. McCullough, *Compos. Part A* 30 (1999) 1.
- [5] T.P. Skourlis, R.L. McCullough, *Compos. Sci. Technol.* 49 (1993) 363.
- [6] J.G. Williams, M.R. James, W.L. Morris, *Compos.* 25 (1994) 757.
- [7] L.T. Drzal, M.J. Rich, M.F. Koenig, P.F. Lloyd, *J. Adhes.* 16 (1983) 133.
- [8] K. Mai, E. Mäder, M. Mühle, *Compos. Part A* 29 (1998) 1111.
- [9] E. Mäder, H.J. Jacobasch, K. Grundke, T. Gietzelt, *Compos. Part A* 27 (1996) 907.
- [10] J.L. Lenhart, J.H. van Zanten, J.P. Dunkers, C.G. Zimba, C.A. James, S.K. Pollack, R.S. Parnas, *J. Colloid Interface Sci.* 221 (2000) 75.
- [11] J.L. Lenhart, J.H. van Zanten, J.P. Dunkers, R.S. Parnas, *Langmuir* 16 (2000) 8145.
- [12] J.L. Lenhart, J.H. van Zanten, J.P. Dunkers, R.S. Parnas, *Macromolecules* 34 (7) (2001) 2225.
- [13] J.P. Dunkers, J.L. Lenhart, S.R. Kueh, J.H. Van Zanten, S.G. Advani, R.S. Parnas, *Opt. Lasers Eng.* 35 (2) (2001) 91–104.
- [14] R.A. Neff, D.L. Woerdeman, R.S. Parnas, *Polym. Compos.* 18 (4) (1997) 518–525.
- [15] D.L. Woerdeman, J.K. Spoerle, K.M. Flynn, R.S. Parnas, *Polym. Compos.* 18 (1997) 133.
- [16] D. Briggs, M.P. Seah, *Practical Surface Analysis by Auger and X-Ray Photoelectron Spectroscopy*, Wiley, New York, 1983, p. 363.
- [17] D.T. Clark, *Adv. Polym. Sci.* 24 (1977) 126.
- [18] J.L. Lenhart, J. Van Zanten, J.P. Dunkers, R.S. Parnas, *Polym. Compos.* 23 (2002) 555.
- [19] L.T. Drzal, in: K. Dusek (Ed.), *Advances in Polymer Science*, Springer-Verlag, Berlin, 1986.

- [20] SPECS GmbH, SpecsLab 1.8.2 Software Manual, 1999, p. 83.
- [21] M.L. Abel, A. Rattana, J.F. Watts, *Langmuir* 16 (16) (2000) 6510.
- [22] K.L. Mittal (Ed.), *Contact Angle, Wettability, and Adhesion*, VSP, Zeist, 1993.
- [23] L.D. White, C.P. Tripp, *J. Colloid Interface Sci.* 232 (2000) 400–407.
- [24] B.C. Bunker, R.W. Carpick, R.A. Assink, M.L. Thomas, M.G. Hankins, J.A. Voigt, D. Sipola, M.P. de Boer, G.L. Gulley, *Langmuir* 16 (2000) 7742–7751.
- [25] M.P. de Boer, T.M. Mayer, T.A. Michalske, U. Srinivasan, R. Maboudian, *Langmuir*, in press.